Observation of Resonant Monopole-Dipole Energy Transfer between Rydberg Atoms and Polar Molecules

J. Zou,[1] R. R. W. Wang,[2,3,*] R. González-Férez,[4] H. R. Sadeghpour,[2] and S. D. Hogan[1,†]
[1]Department of Physics and Astronomy, University College London, Gower Street, London WC1E 6BT, United Kingdom
[2]ITAMP, Center for Astrophysics | Harvard & Smithsonian, Cambridge, Massachusetts 02138, USA
[3]Department of Physics, Harvard University, Cambridge, Massachusetts 02138, USA
[4]Instituto Carlos I de Física Teórica y Computacional, and Departamento de Física Atómica, Molecular y Nuclear, Universidad de Granada, 18071 Granada, Spain

(Received 25 September 2025; accepted 12 February 2026; published 20 March 2026)

Resonant energy transfer (RET) between the equal parity 1s65s $^3S_1$ and 1s66s $^3S_1$ Rydberg levels in helium has been observed in low-temperature (∼80 mK) collisions with ammonia molecules that undergo inversion transitions in their X $^1A_1$ ground electronic state. This hybrid Rydberg-atom–polar-molecule resonant energy transfer represents a monopole-dipole energy exchange reaction that necessarily requires spatial overlap of the Rydberg-electron and molecular wave functions. Calculations that account explicitly for the charge-dipole interaction between the Rydberg electron and the molecule provide a quantitative explanation of the observations. Total parity is conserved in the reaction through the mixing of collisional angular momentum in the atom-molecule complex. This work opens opportunities to expand the toolbox for quantum science with charge-dipole-mediated energy exchange in hybrid atom–polar-molecule platforms.

DOI: 10.1103/k9d5-1jcc

Resonant energy transfer (RET), the phenomenon by which an excitation is exchanged between energetically resonant quantum states, is of widespread interest in physics, chemistry, and biology [1]. It was first discussed by Förster [2] in the context of energy migration in dye polymers. Since pioneering experiments of Cario and Frank [3], RET has been utilized to explain photosynthesis in light harvesting complexes [4,5], for imaging at single-molecule resolution [6], to tune molecular interactions and suppress chemical reactions [7,8], and to enrich the toolbox for quantum information processing [9–11].

Förster RET, which relies on the interaction between electric dipole transition moments [2,12–14], has been studied in cold dilute gases with Rydberg-Rydberg [15–17], Rydberg–polar-molecule [18–22], and molecule-molecule [23,24] interactions. Beyond dipolar interactions, RET can also be associated with higher-order multipole transition moments, as evident, e.g., from observations of RET due to dipole-quadrupole couplings [25–27]. There is currently growing interest in RET between Rydberg atoms and polar ground-state molecules since the hybridization of these two platforms for quantum information processing, through resonant exchange interactions, would allow, e.g., rotational states in the molecules to be exploited as long-coherence-time quantum memories with initialization or readout through the atoms [28,29].

Here, we report the observation of a RET process that involves a monopole transition in a Rydberg atom and an electric dipole transition in a polar molecule. The term "monopole" here refers to an electronic transition between equal parity Rydberg states, both of which have zero electron orbital angular momentum, and not to the order of expansion in the charge distribution. Specifically, this involves the $|65s\rangle \leftrightarrow |66s\rangle$ transition between equal parity triplet Rydberg states in He ($|ns\rangle \equiv |1s ns\, ^3S_1\rangle$), and the opposite-parity states of the inversion doublet, $|\pm\rangle$, in ammonia (NH_3) [X $^1A_1(J = K = 1)$, where J and K are the rotational quantum numbers]. The single-photon transition between these Rydberg states is forbidden by both electric dipole and quadrupole selection rules. Consequently, RET between these systems must be accompanied by a change in collisional angular momentum to conserve total parity. From the perspective of the composite system comprising the polar molecule located inside the Rydberg orbital, the results presented here are analogous to electric-monopole transitions associated with internal conversion in atomic nuclei [30,31]. They represent, to our knowledge, the first observation of RET in a cold neutral gas that does not rely on interactions at large interparticle separations.

*Contact author: reuben.wang@cfa.harvard.edu
†Contact author: s.hogan@ucl.ac.uk

Published by the American Physical Society under the terms of the Creative Commons Attribution 4.0 International license. Further distribution of this work must maintain attribution to the author(s) and the published article's title, journal citation, and DOI.

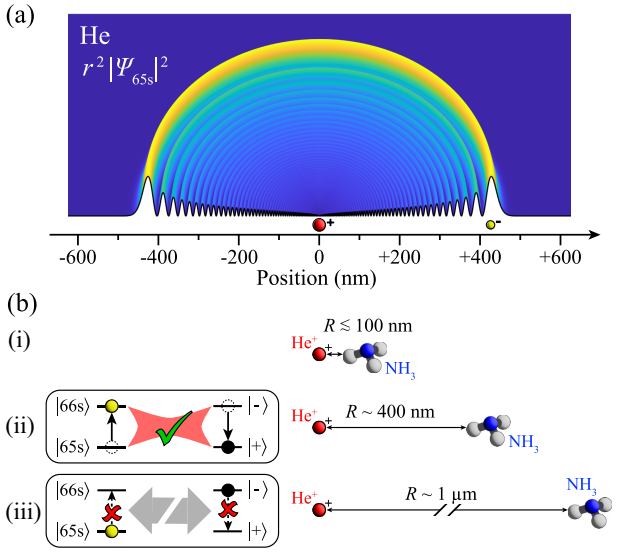


FIG. 1. (a) Electron charge distribution in the $|65s\rangle$ orbital in He. (b) Distance scales associated with the interaction of a Rydberg He atom and an NH_3 molecule at which the interaction of the molecule with the (i) He^+ ion core, (ii) Rydberg electron, and (iii) composite neutral atom dominate. The resonant monopole-dipole energy transfer reported here is forbidden at large distances (iii, left), but can occur at intermediate distances because of the charge-dipole interaction with the Rydberg electron (ii, left).

When a Rydberg atom and a neutral molecule are far apart, as in Fig. 1(b)(iii), they interact *via* far-field electrostatic interactions, either by first order induced or permanent dipole moments, or second order dispersion interactions, leading to level shifts, excitation blockade, and, under appropriate conditions, RET [17,22,24]. When a polar molecule is near the outer lobe of the Rydberg-electron charge distribution [compare Figs. 1(a) and (b)(ii)], charge-dipole interactions dominate. Within the Rydberg electron orbit, these interactions must be treated in the near field where the Rydberg atom is no longer a point charge distribution [32–35]. Finally, when the molecule is further inside the Rydberg electron charge distribution [Fig. 1(b)(i)], it interacts predominantly with the ion core, often leading to barrierless exothermic ion-molecule reactions [36]. This region we simply refer to here as "short distances."

We show here that the interaction of a Rydberg electron with the dipole moment of a polar molecule can mediate resonant monopole-dipole energy transfer. The theory that describes this RET also explains how off-resonant energy transfer between the same pair of molecular states, and the $|65s\rangle \leftrightarrow |64s\rangle$ transition in He is suppressed. This Letter demonstrates a new probe of atom-molecule interactions at mesoscopic scales (on the order of hundreds of nanometers), expanding the toolbox for quantum information processing in hybrid Rydberg-atom–molecule platforms.

The experiments were performed in an intrabeam collision apparatus with pulsed supersonic beams containing pure He, or a mixture of NH_3 and He (1:63 by pressure) [37]. The He atoms were prepared in the metastable $1s2s\ ^3S_1$ level using a dc electric discharge [38]. After collimation and the removal of charge particles, the atoms were excited to $|ns\rangle$ Rydberg states ($64 \leq n \leq 67$) using the resonance-enhanced two-color two-photon $1s2s\,^3S_1 \rightarrow 1s3p\,^3P_2 \rightarrow 1sns\,^3S_1$ scheme [39]. With the NH_3 in the beam, the molecule number density was $(1.5 \pm 0.4) \times 10^{10}$ cm^{-3} at the Rydberg state photoexcitation position, and the mean center-of-mass collision speed between the atoms and the molecules was 19.3 ± 2.6 m/s [20]. Consequently, the relative translational temperature at which atom-molecule collisions occurred was $E_{\rm kin}/k_B \sim 80$ mK ($E_{\rm kin}/h \sim 1.6$ GHz or $E_{\rm kin}/hc \sim 0.055$ cm^{-1}), with $E_{\rm kin}$ the center-of-mass collision energy.

Following photoexcitation, the cold Rydberg atoms and the molecules evolved in nominally zero electric field for up to 12 μs. Then, a slowly-rising electric field pulse was applied to ionize the Rydberg atoms. In this field, atoms in states with higher (lower) values of n ionized at earlier (later) times. Consequently, the arrival time of the ionized electrons at a microchannel plate detector could be correlated with their ionization field, and the value of n of the states populated. Stray electric fields in the interaction region of the apparatus were canceled to < 20 mV/cm by microwave spectroscopy of the single-color two-photon $|65s\rangle \rightarrow |63s\rangle$ transition (see Appendix B).

Resonant monopole-dipole energy transfer—To probe resonant monopole-dipole energy transfer between the molecules and atoms, data were recorded with He atoms prepared in selected $|ns\rangle$ states. In the absence of NH_3, this resulted in the set of separated electric field ionization features with maxima at fields from ~22.5–19 V/cm indicated by the thin continuous black curves in Fig. 2(a). With the molecules present (thick red curves), the normalized ionization profiles obtained following preparation of the $|64s\rangle$ and $|67s\rangle$ states maintain a similar structure, but some depletion is observed. This is a result of electric-dipole-allowed rotational energy transfer to Rydberg states with values of $n > 100$ [40], as seen in Fig. 3(a) where a broader range of ionization fields are spanned. However, for the $|65s\rangle$ and $|66s\rangle$ states the situation is different. For atoms in the $|65s\rangle$ state in Fig. 2(a), an appreciable electron signal is apparent in the region labeled A. This results from population transfer to the $|66s\rangle$ state. A fit of the sum of two Gaussian functions (dashed green and dash-dotted blue curves) constrained by the fits to the pure-He reference data, yields a transfer rate of $17 \pm 5\%$ from the $|65s\rangle$ state to the $|66s\rangle$ state, which are separated by 23.735 GHz. A similar behavior is seen upon preparation of atoms in the $|66s\rangle$ state, with $16 \pm 5\%$ population transfer to the $|65s\rangle$ state.

The data in Fig. 2 demonstrate a resonant transfer of energy involving the $|-\rangle \leftrightarrow |+\rangle$ electric-dipole-allowed inversion transition in NH_3 at 23.695 GHz [41] (these states

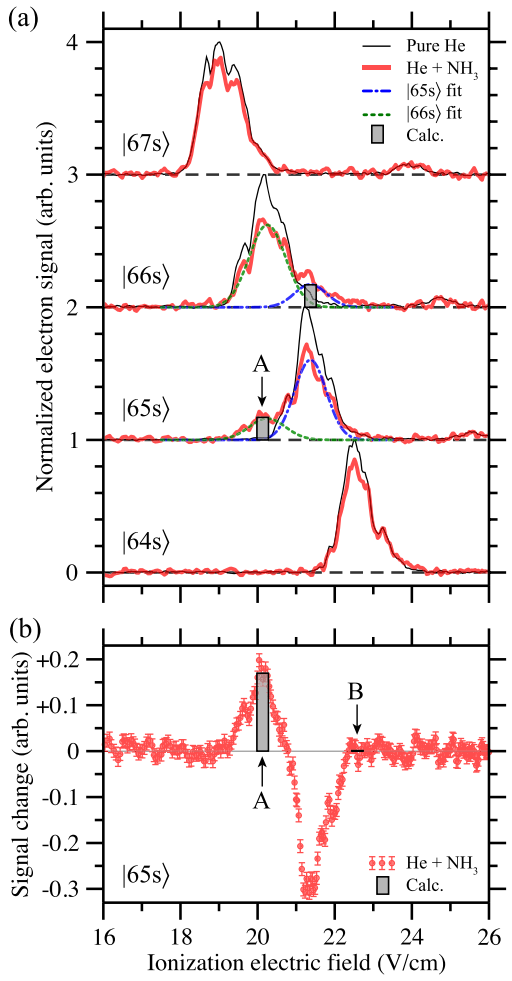


FIG. 2. (a) Electron signals recorded following excitation of He atoms to selected $|ns\rangle$ Rydberg states in the absence (thin black curves) and presence (thick red curves) of NH_3. The horizontal axis indicates the electric field in which the Rydberg atoms ionized. The calculated population transfer for atoms initially prepared in the $|65s\rangle$ and $|66s\rangle$ states in the presence of NH_3 [$\mathbb{P}(|65s,-\rangle \rightarrow |66s,+\rangle) \approx 17\%$] is indicated by the vertical bars. (b) Difference between the electron signals recorded without and with NH_3 present for atoms prepared in the $|65s\rangle$ state, with the calculated resonant (off-resonant) population transfer to the $|66s\rangle$ ($|64s\rangle$) state labeled A (B) [$\mathbb{P}(|65s,+\rangle \rightarrow |64s,-\rangle) \approx 0.12\%$]. Note: the uncertainty in the calculations is not shown but is comparable to the uncertainty on the experimental data points.

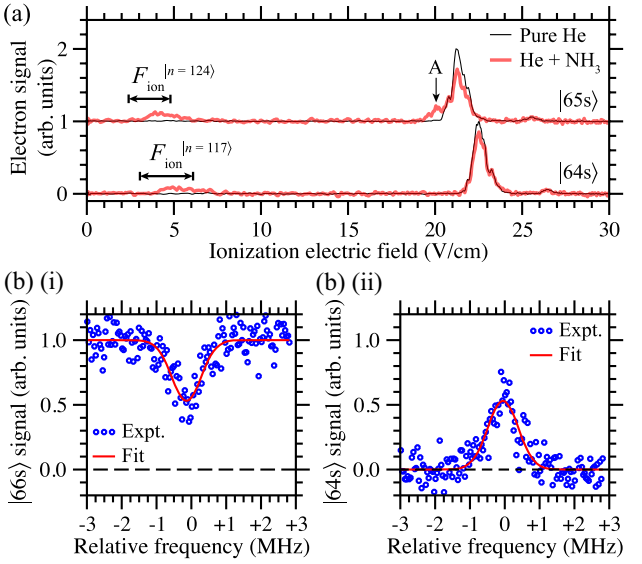


FIG. 3. (a) Broad view of the ionization signals in Fig. 2 for atoms prepared in the $|64s\rangle$ and $|65s\rangle$ states with (red) and without (black) NH_3. $F_{\mathrm{ion}}^{|n\rangle}$ denotes the range of ionization electric fields of the high-n hydrogenic Rydberg states populated by electric-dipole-allowed rotational energy (~572 GHz) transfer from the NH_3. (b) Microwave spectra of the single-color two-photon $|66s\rangle \rightarrow |64s\rangle$ transition in atoms that underwent RET from the $|65s\rangle$ state following collisions with NH_3. The microwave frequency is displayed with respect to the field-free two-photon transition frequency of 24.298 146 GHz.

are equally populated in the supersonic beam), and the $|65s\rangle \leftrightarrow |66s\rangle$ transition in He. This seemingly violates parity conservation because it involves a pair of equal parity Rydberg levels, but molecular states with opposite parity. Nevertheless, we confirm that the $|66s\rangle$ state is indeed selectively populated in this process by high-resolution microwave spectroscopy of atoms that underwent energy transfer. This was implemented by applying a 2-μs-duration microwave pulse to probe the atoms using the single-color two-photon $|66s\rangle \rightarrow |64s\rangle$ transition at $2 \times 24.298\,146$ GHz, after an interaction time of 5 μs with the molecules, while monitoring the $|66s\rangle$ and $|64s\rangle$ electron signals. The resulting spectra are shown in Fig. 3(b). Gaussian functions fit to these data (continuous red curves) indicate that the measured transition frequency of 24.298 050(41) GHz is -96 ± 41 kHz below the field-free transition frequency. We attribute this shift to a residual stray electric field of 16.5 ± 4.5 mV/cm in the interaction region of the apparatus. This stray field induces a negligible ($< 0.03\%$) admixture of $|np\rangle$ character into the $|ns\rangle$ states, and is therefore not primarily responsible for the observed energy transfer (see Appendix B). While all previous observations of RET have been interpreted through interactions occurring between the particles in the far field, here, the resonant monopole-dipole (Rydberg-atom–polar-molecule) energy transfer is mediated by near-field interactions of the Rydberg electron with the molecular dipole.

Charge-dipole mediated RET—The anisotropic charge-dipole interaction potential has the form [32]

$$V_{\mathrm{CD}}(\boldsymbol{r},\boldsymbol{R}) = -\boldsymbol{\mu}_{\mathrm{NH_3}} \cdot \boldsymbol{\mathcal{E}}_{\mathrm{Ryd}}(\boldsymbol{r},\boldsymbol{R}), \tag{1}$$

where $\boldsymbol{R}$ is the coordinate between the molecule and the He^+ ion core, and

$$\boldsymbol{\mathcal{E}}_{\mathrm{Ryd}}(\boldsymbol{r},\boldsymbol{R}) = \frac{e}{4\pi\epsilon_0}\left(\frac{\boldsymbol{R}}{R^3} - \frac{\boldsymbol{R}-\boldsymbol{r}}{|\boldsymbol{R}-\boldsymbol{r}|^3}\right) \tag{2}$$

is the electric field generated by the He^+ ion and the Rydberg electron at position $\boldsymbol{r}$, and $\boldsymbol{\mu}_{NH_3}$ is the electric dipole operator coupling opposite parity states in NH_3. The charge-dipole interaction scales as $1/R^2$ and is in fact long-ranged. However, as shown below, it becomes important at near-field distances ($\lesssim$400 nm in the case considered here), when the molecule is located inside the Rydberg-electron charge distribution. In this situation, for the triplet $\ell = 0$ Rydberg states in He with an energy splitting that is closest to resonance with the NH_3 inversion interval, this electron-molecule interaction is dominated by the monopole term. This term is nonzero because the corresponding integral only extends over a restricted range, i.e., $0 < r < R$ (see Appendix A and Supplemental Material [42]).

The adiabatic potential curves (adiabats) that connect to the $|65s, -\rangle$ and $|66s, +\rangle$ states asymptotically are shown in Fig. 4(a) (continuous curves). When compared to the diabatic potentials (dashed curves which neglect off-diagonal couplings) that cross at $R \approx 110$ nm, the charge-dipole interaction induces a strong level repulsion in the adiabats between the $|65s, -\rangle$ and $|66s, +\rangle$ states [blue curve in Fig. 4(b)]. Collisional RET between the two adiabats occurs nonadiabatically over the interaction region (see Appendix A).

The transition rate $\Gamma(|i\rangle \to |f\rangle)$ for RET between an initial (final) state $|i\rangle = |65s, -\rangle$ ($|f\rangle = |66s, +\rangle$) is obtained by considering the product of the NH_3 number density, n_{NH_3}, and the thermally averaged rate constant $\beta(|i\rangle \to |f\rangle) = \int (\hbar K/\mu)\sigma_{|i\rangle\to|f\rangle} c_{MB}(\boldsymbol{K}) d^3\boldsymbol{K}$, where $c_{MB}(\boldsymbol{K})$

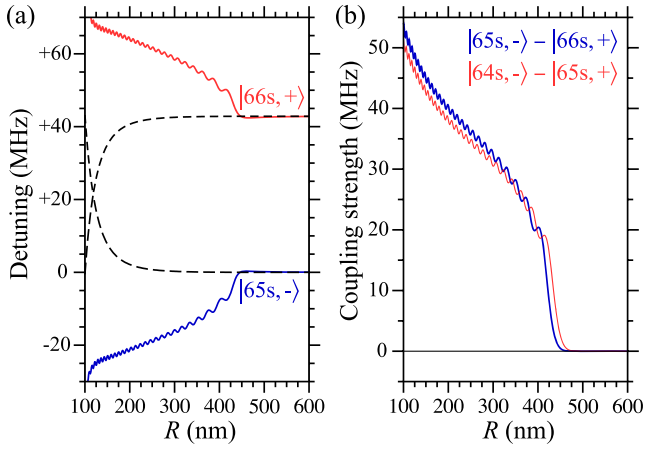


FIG. 4. (a) Adiabatic (continuous curves) and diabatic (dashed curves) atom-molecule interaction potentials as a function of internuclear distance R. The curves corresponding to the $|65s, -\rangle$ and $|66s, +\rangle$ asymptotic eigenstates are indicated. The hybridization of the opposite parity molecular states becomes appreciable only near the outer turning point of the Rydberg-electron wave function ($R \sim 400$ nm) because of the enhanced charge-dipole interaction. (b) The coupling matrix element between the $|65s, -\rangle$ and $|66s, +\rangle$ states (continuous dark blue curve), and $|64s, -\rangle$ and $|65s, +\rangle$ states (continuous light red curve) as a function of R.

is a Maxwell-Boltzmann distribution of collision momenta. At collision energies much larger than the transition-state detuning $\Delta_{i,f}$, the scattering cross section, treated within the Born approximation [49], is

$$\sigma_{|i\rangle\to|f\rangle} = \frac{\pi}{K_i^2}|T_{|i\rangle\to|f\rangle}|^2, \tag{3}$$

with the transition T matrix

$$T_{|i\rangle\to|f\rangle} \approx \frac{16i\pi^2\mu}{\hbar^2\sqrt{K_i K_f}}\left(1 - \sqrt{\frac{2\mu\Delta_{i,f}}{\hbar^2 K_i^2}}\right) \times \int \langle f|V_{CD}(R)|i\rangle \cos\left[(K_f - K_i)R\right] dR, \tag{4}$$

where μ is the reduced mass and $K_\nu = \sqrt{2\mu(E - \varepsilon_\nu)/\hbar^2}$ is the wave number corresponding to the collision threshold ε_ν, with $\nu = i, f$ (see Supplemental Material for further details [42]). The T-matrix element above implies that the efficacy of collisional RET is determined by the detuning of K_f from K_i. Larger detunings result in more rapidly oscillating integrands, which suppress the RET cross section.

Considering the experimental conditions, for which the interaction time of the mixture of Rydberg He atoms and NH_3 molecules was $\Delta t = 12$ μs, the calculated probability $\mathbb{P}(|65s, -\rangle \to |66s, +\rangle) = 1 - e^{-\Gamma\Delta t}$, that any given He atom undergoes RET to the $|66s\rangle$ state is found to be $17 \pm 4\%$. This is represented by the vertical bars in Fig. 2(a). The uncertainty on this theoretical quantity results from propagation of the error in the number density and collision speed in the experiments. Similarly, we compute the nonresonant monopole-dipole induced population transfer between the $|65s, +\rangle$ and $|64s, -\rangle$ states to be $\mathbb{P}(|65s, +\rangle \to |64s, -\rangle) \approx 0.12 \pm 0.03\%$.

Despite similar charge-dipole coupling strengths between the $|65s, -\rangle$ and $|66s, +\rangle$ states, and the $|65s, +\rangle$ and $|64s, -\rangle$ states [Fig. 4(b)], the latter energy transfer process is highly suppressed because the $|65s, +\rangle \leftrightarrow |64s, -\rangle$ detuning of $\Delta_{i,f} = 1.166$ GHz is more than an order of magnitude larger than the $|65s, -\rangle \leftrightarrow |66s, +\rangle$ detuning ($\Delta_{i,f} = 0.040$ GHz). Direct comparison of these results with the experimental data is seen in Fig. 2(b). These data represent the difference between the normalized electric field ionization signals recorded following preparation of the $|65s\rangle$ state with and without NH_3. The dip observed close to 21 V/cm corresponds to the depletion of the $|65s\rangle$ population by RET. The enhancement in the signal in the region labeled A, represents the resonant monopole-dipole energy transfer to the $|66s\rangle$ state with the observed population transfer in excellent quantitative agreement with the calculations (vertical bar). The calculated value of $\mathbb{P}(|65s, +\rangle \to |64s, -\rangle)$ is indicated by the small black bar labeled B at 22.5 V/cm. The calculated transfer in this case is below the experimental sensitivity.

The theoretical treatment therefore corroborates the experimental observation of resonant monopole-dipole energy transfer. The resonant nature of this process, which is only seen at $n = 65$ and 66, shows that the ionization signals do not arise as a result of short-range He^+-ion–dipole chemistry [36].

Parity conservation—It is notable that the $|65s, -\rangle$ and $|66s, +\rangle$ pair states both comprise even parity Rydberg levels, while the inversion sublevels in NH_3 have opposite parity. The conservation of the total parity symmetry of the collision complex must, therefore, be enforced through the relative mechanical angular momentum [26]. The requisite coupling between opposite parity collisional partial waves $|L, m_L\rangle$, occurs through the anisotropy of the charge-dipole interaction, which is proportional to $\cos\theta_R$, with θ_R the angle between the molecular dipole and collision coordinate [42]. At the collision energies in the experiments, a large number of collisional partial waves ($L \approx 200$) are involved [42], making it difficult to resolve the partial wave parity change. However, this may be observed in the future in differential scattering experiments in the ultracold regime close to the *s*-wave limit [7,50,51].

Conclusion—We have observed resonant monopole-dipole energy transfer between equal parity Rydberg levels in He, and the ground-state inversion doublet in NH_3. This resonant energy exchange is mediated by the charge-dipole interaction of the Rydberg electron with the polar molecule, which leads to the hybridization of the opposite parity inversion sublevels in NH_3. Total parity is conserved by the admixture of collisional angular momenta of the atom-molecule complex. The theoretical treatment of the $He(|ns\rangle)$-NH_3 encounters, as charge-dipole-mediated scattering events, is in excellent quantitative agreement with the measured state-to-state population transfer. The theory also provides insight into the suppression of nonresonant transition probabilities in such collisions.

Whereas all Förster RET processes identified up to now could be treated at far-field distances, we expect the resonant monopole-dipole energy transfer observed here to be a universal feature of charge-dipole interacting quantum systems in the near field. It is not restricted to He Rydberg atoms and NH_3 molecules, nor does it necessarily rely on the coupling to the molecule nuclear motion degree of freedom exploited here. We envision that it could be observed in ultracold gases, expanding the range of tunable interactions available in hybrid atom-molecule platforms. Zeeman shifts of the Rydberg levels may be exploited to allow selected monopole transitions to be fined-tuned into resonance with an electric-dipole transition of the interacting partner without inducing longer-range interactions. Such control over the resonance condition presents resonant monopole-dipole energy transfer as a powerful tool for spin-motion coupled quantum applications [11,52–55].

The association of Rydberg atoms and polar molecules into giant polyatomic Rydberg molecules [33,56,57] might also allow for continuous coherent oscillations between resonant Rydberg and molecular states, without the need for external confinement. Moreover, recent advances in optical tweezer techniques to control and trap neutral atoms and molecules [58–64] may permit on-demand access to monopole-dipole blockade [65,66] or antiblockade [67,68] physics for quantum simulation and computing.

Acknowledgments—This work is supported by the UK Science and Technology Facilities Research Council under Grant No. ST/T006439/1. R. R. W. W. and H. R. S. acknowledge support at ITAMP from the National Science Foundation, and R. G. F. acknowledges support from the Spanish project PID2023-147039NB-I00 (MICIN).

Data availability—The data that support the findings of this article are not publicly available upon publication because it is not technically feasible and/or the cost of preparing, depositing, and hosting the data would be prohibitive within the terms of this research project. The data are available from the authors upon reasonable request.

[1] G. A. Jones and D. S. Bradshaw, Resonance energy transfer: From fundamental theory to recent applications, Front. Phys. **7**, 100 (2019).
[2] T. Forster, Energiewanderung und Fluoreszenz, Naturwissenschaften **33**, 166 (1946).
[3] G. Cario and J. Franck, Über Zerlegung von Wasserstoffmolekülen durch angeregte Quecksilberatome, Z. Phys. **11**, 161 (1922).
[4] M. Şener, J. Strümpfer, J. Hsin, D. Chandler, S. Scheuring, C. N. Hunter, and K. Schulten, Förster energy transfer theory as reflected in the structures of photosynthetic light-harvesting systems, Chem. Phys. Chem. **12**, 518 (2011).
[5] T. Mirkovic, E. E. Ostroumov, J. M. Anna, R. van Grondelle, Govindjee, and G. D. Scholes, Light absorption and energy transfer in the antenna complexes of photosynthetic organisms, Chem. Rev. **117**, 249 (2017).
[6] T. Ha, J. Fei, S. Schmid, N. K. Lee, R. L. Gonzalez, S. Paul, and S. Yeou, Fluorescence resonance energy transfer at the single-molecule level, Nat. Rev. Methods Primers **4**, 21 (2024).
[7] J.-R. Li, W. G. Tobias, K. Matsuda, C. Miller, G. Valtolina, L. De Marco, R. R. W. Wang, L. Lassablière, G. Quéméner, J. L. Bohn, and J. Ye, Tuning of dipolar interactions and evaporative cooling in a three-dimensional molecular quantum gas, Nat. Phys. **17**, 1144 (2021).
[8] L. Lassablière and G. Quéméner, Model for two-body collisions between ultracold dipolar molecules around a Förster resonance in an electric field, Phys. Rev. A **106**, 033311 (2022).
[9] A. N. Carroll, H. Hirzler, C. Miller, D. Wellnitz, S. R. Muleady, J. Lin, K. P. Zamarski, R. R. W. Wang, J. L. Bohn, A. M. Rey, and J. Ye, Observation of generalized *t-J* spin dynamics with tunable dipolar interactions, Science **388**, 381 (2025).

[10] A. Guttridge, D. K. Ruttley, A. C. Baldock, R. González-Férez, H. R. Sadeghpour, C. S. Adams, and S. L. Cornish, Observation of Rydberg blockade due to the charge-dipole interaction between an atom and a polar molecule, Phys. Rev. Lett. **131**, 013401 (2023).
[11] L. R. B. Picard, A. J. Park, G. E. Patenotte, S. Gebretsadkan, D. Wellnitz, A. M. Rey, and K.-K. Ni, Entanglement and iSWAP gate between molecular qubits, Nature (London) **637**, 821 (2025).
[12] J. Perrin, Fluorescence et induction moléculaire par résonance, C. R. Hebd. Séances Acad. Sci. **184**, 1097 (1927).
[13] H. Kallmann and F. London, Über quantenmechanische Energieübertragung zwischen atomaren Systemen, Z. Phys. Chem. **2B**, 207 (1929).
[14] F. Perrin, Théorie quantique des transferts d'activation entre molécules de même espèce. Cas des solutions fluorescentes, Ann. Phys. (N.Y.) **10**, 283 (1932).
[15] C. S. E. van Ditzhuijzen, A. F. Koenderink, J. V. Hernández, F. Robicheaux, L. D. Noordam, and H. B. van Linden van den Heuvell, Spatially resolved observation of dipole-dipole interaction between Rydberg atoms, Phys. Rev. Lett. **100**, 243201 (2008).
[16] S. Ravets, H. Labuhn, D. Barredo, L. Béguin, T. Lahaye, and A. Browaeys, Coherent dipole–dipole coupling between two single Rydberg atoms at an electrically-tuned Förster resonance, Nat. Phys. **10**, 914 (2014).
[17] S. de Léséleuc, D. Barredo, V. Lienhard, A. Browaeys, and T. Lahaye, Optical control of the resonant dipole-dipole interaction between Rydberg atoms, Phys. Rev. Lett. **119**, 053202 (2017).
[18] V. Zhelyazkova and S. D. Hogan, Electrically tuned Förster resonances in collisions of NH_3 with Rydberg He atoms, Phys. Rev. A **95**, 042710 (2017).
[19] F. Jarisch and M. Zeppenfeld, State resolved investigation of Förster resonant energy transfer in collisions between polar molecules and Rydberg atoms, New J. Phys. **20**, 113044 (2018).
[20] J. Zou and S. D. Hogan, Probing van der Waals interactions and detecting polar molecules by Förster-resonance energy transfer with Rydberg atoms at temperatures below 100 mK, Phys. Rev. A **106**, 043111 (2022).
[21] S. Patsch, M. Zeppenfeld, and C. P. Koch, Rydberg atom-enabled spectroscopy of polar molecules via Förster resonance energy transfer, J. Phys. Chem. Lett. **13**, 10728 (2022).
[22] L. Zhu, J. Luke, R. Shaham, Y.-X. Liu, and K.-K. Ni, Probing dipolar interactions between Rydberg atoms and ultracold polar molecules, Phys. Rev. Lett. **135**, 153001 (2025).
[23] B. Yan, S. A. Moses, B. Gadway, J. P. Covey, K. R. A. Hazzard, A. M. Rey, D. S. Jin, and J. Ye, Observation of dipolar spin-exchange interactions with lattice-confined polar molecules, Nature (London) **501**, 521 (2013).
[24] L. Christakis, J. S. Rosenberg, R. Raj, S. Chi, A. Morningstar, D. A. Huse, Z. Z. Yan, and W. S. Bakr, Probing site-resolved correlations in a spin system of ultracold molecules, Nature (London) **614**, 64 (2023).
[25] T. F. Gallagher, G. A. Ruff, and K. A. Safinya, Resonant electronic to vibrational energy transfer from Na to CH_4 and CD_4, Phys. Rev. A **22**, 843 (1980).
[26] J. Deiglmayr, H. Saßmannshausen, P. Pillet, and F. Merkt, Observation of dipole-quadrupole interaction in an ultracold gas of Rydberg atoms, Phys. Rev. Lett. **113**, 193001 (2014).
[27] W. Maineult, B. Pelle, R. Faoro, E. Arimondo, P. Pillet, and P. Cheinet, Dipole–quadrupole Förster resonance in cesium Rydberg gas, J. Phys. B **49**, 214001 (2016).
[28] K. Wang, C. P. Williams, L. R. B. Picard, N. Y. Yao, and K.-K. Ni, Enriching the quantum toolbox of ultracold molecules with Rydberg atoms, PRX Quantum **3**, 030339 (2022).
[29] C. Zhang and M. R. Tarbutt, Quantum computation in a hybrid array of molecules and Rydberg atoms, PRX Quantum **3**, 030340 (2022).
[30] E. L. Church and J. Weneser, Electric-monopole transitions in atomic nuclei, Phys. Rev. **103**, 1035 (1956).
[31] S. Zerguine, P. Van Isacker, A. Bouldjedri, and S. Heinze, Correlating radii and electric monopole transitions of atomic nuclei, Phys. Rev. Lett. **101**, 022502 (2008).
[32] E. Kuznetsova, S. T. Rittenhouse, H. R. Sadeghpour, and S. F. Yelin, Rydberg-atom-mediated nondestructive readout of collective rotational states in polar-molecule arrays, Phys. Rev. A **94**, 032325 (2016).
[33] S. T. Rittenhouse and H. R. Sadeghpour, Ultracold giant polyatomic Rydberg molecules: Coherent control of molecular orientation, Phys. Rev. Lett. **104**, 243002 (2010).
[34] M. Schlagmüller, T. C. Liebisch, F. Engel, K. S. Kleinbach, F. Böttcher, U. Hermann, K. M. Westphal, A. Gaj, R. Löw, S. Hofferberth, T. Pfau, J. Pérez-Ríos, and C. H. Greene, Ultracold chemical reactions of a single Rydberg atom in a dense gas, Phys. Rev. X **6**, 031020 (2016).
[35] P. Geppert, M. Althön, D. Fichtner, and H. Ott, Diffusive-like redistribution in state-changing collisions between Rydberg atoms and ground state atoms, Nat. Commun. **12**, 3900 (2021).
[36] V. Zhelyazkova, F. B. V. Martins, J. A. Agner, H. Schmutz, and F. Merkt, Multipole-moment effects in ion–molecule reactions at low temperatures: Part I—ion-dipole enhancement of the rate coefficients of the $He^+ + NH_3$ and $He^+ + ND_3$ reactions at collisional energies E_{coll}/k_B near 0 K, Phys. Chem. Chem. Phys. **23**, 21606 (2021).
[37] K. Gawlas and S. D. Hogan, Rydberg-state-resolved resonant energy transfer in cold electric-field-controlled intra-beam collisions of NH_3 with Rydberg He atoms, J. Phys. Chem. Lett. **11**, 83 (2020).
[38] T. Halfmann, J. Koensgen, and K. Bergmann, A source for a high-intensity pulsed beam of metastable helium atoms, Meas. Sci. Technol. **11**, 1510 (2000).
[39] S. D. Hogan, Y. Houston, and B. Wei, Laser photoexcitation of Rydberg states in helium with $n > 400$, J. Phys. B **51**, 145002 (2018).
[40] K. A. Smith, F. G. Kellert, R. D. Rundel, F. B. Dunning, and R. F. Stebbings, Discrete energy transfer in collisions of $Xe(nf)$ Rydberg atoms with NH_3 molecules, Phys. Rev. Lett. **40**, 1362 (1978).
[41] J. W. Simmons and W. Gordy, Structure of the inversion spectrum of ammonia, Phys. Rev. **73**, 713 (1948).
[42] See Supplemental Material at http://link.aps.org/supplemental/10.1103/k9d5-1jcc for collision theory of charge-dipole mediated RET, which includes Refs. [43–48].

[43] E. Fermi and E. Teller, The capture of negative mesotrons in matter, Phys. Rev. **72**, 399 (1947).
[44] G. W. F. Drake, High precision theory of atomic helium, Phys. Scr. **1999**, 83 (1999).
[45] S. Green, Energy transfer in NH_3-He collisions, J. Chem. Phys. **73**, 2740 (1980).
[46] A. P. Hickman, Theory of angular momentum mixing in Rydberg-atom-rare-gas collisions, Phys. Rev. A **18**, 1339 (1978).
[47] A. P. Hickman, Relation between low-energy-electron scattering and ℓ-changing collisions of Rydberg atoms, Phys. Rev. A **19**, 994 (1979).
[48] A. Tsikritea, J. A. Diprose, T. P. Softley, and B. R. Heazlewood, Capture theory models: An overview of their development, experimental verification, and applications to ion–molecule reactions, J. Chem. Phys. **157**, 060901 (2022).
[49] M. Matsuzawa, State-changing collision of a high-Rydberg atom with a polar molecule, Phys. Rev. A **20**, 860 (1979).
[50] K. Aikawa, A. Frisch, M. Mark, S. Baier, R. Grimm, J. L. Bohn, D. S. Jin, G. M. Bruun, and F. Ferlaino, Anisotropic relaxation dynamics in a dipolar Fermi gas driven out of equilibrium, Phys. Rev. Lett. **113**, 263201 (2014).
[51] R. R. W. Wang and J. L. Bohn, Anisotropic thermalization of dilute dipolar gases, Phys. Rev. A **103**, 063320 (2021).
[52] J. Mizrahi, C. Senko, B. Neyenhuis, K. G. Johnson, W. C. Campbell, C. W. S. Conover, and C. Monroe, Ultrafast spin-motion entanglement and interferometry with a single atom, Phys. Rev. Lett. **110**, 203001 (2013).
[53] A. Dareau, Y. Meng, P. Schneeweiss, and A. Rauschenbeutel, Observation of ultrastrong spin-motion coupling for cold atoms in optical microtraps, Phys. Rev. Lett. **121**, 253603 (2018).
[54] V. Bharti, S. Sugawa, M. Kunimi, V. S. Chauhan, T. P. Mahesh, M. Mizoguchi, T. Matsubara, T. Tomita, S. de Léséleuc, and K. Ohmori, Strong spin-motion coupling in the ultrafast dynamics of Rydberg atoms, Phys. Rev. Lett. **133**, 093405 (2024).
[55] R. R. W. Wang and J. L. Bohn, Theory of itinerant collisional spin dynamics in nondegenerate molecular gases, Phys. Rev. A **112**, 043315 (2025).
[56] R. González-Férez, H. R. Sadeghpour, and P. Schmelcher, Rotational hybridization, and control of alignment and orientation in triatomic ultralong-range Rydberg molecules, New J. Phys. **17**, 013021 (2015).
[57] V. Bendkowsky, B. Butscher, J. Nipper, J. P. Shaffer, R. Löw, and T. Pfau, Observation of ultralong-range Rydberg molecules, Nature (London) **458**, 1005 (2009).
[58] L. Anderegg, L. W. Cheuk, Y. Bao, S. Burchesky, W. Ketterle, K.-K. Ni, and J. M. Doyle, An optical tweezer array of ultracold molecules, Science **365**, 1156 (2019).
[59] L. Anderegg, S. Burchesky, Y. Bao, S. S. Yu, T. Karman, E. Chae, K.-K. Ni, W. Ketterle, and J. M. Doyle, Observation of microwave shielding of ultracold molecules, Science **373**, 779 (2021).
[60] D. Bluvstein, H. Levine, G. Semeghini, T. T. Wang, S. Ebadi, M. Kalinowski, A. Keesling, N. Maskara, H. Pichler, M. Greiner, V. Vuletić, and M. D. Lukin, A quantum processor based on coherent transport of entangled atom arrays, Nature (London) **604**, 451 (2022).
[61] D. K. Ruttley, A. Guttridge, S. Spence, R. C. Bird, C. R. Le Sueur, J. M. Hutson, and S. L. Cornish, Formation of ultracold molecules by merging optical tweezers, Phys. Rev. Lett. **130**, 223401 (2023).
[62] D. K. Ruttley, A. Guttridge, T. R. Hepworth, and S. L. Cornish, Enhanced quantum control of individual ultracold molecules using optical tweezer arrays, PRX Quantum **5**, 020333 (2024).
[63] D. K. Ruttley, T. R. Hepworth, A. Guttridge, and S. L. Cornish, Long-lived entanglement of molecules in magic-wavelength optical tweezers, Nature (London) **637**, 827 (2025).
[64] A. Guttridge, T. R. Hepworth, D. K. Ruttley, A. A. T. Durst, M. T. Eiles, and S. L. Cornish, Individual assembly of two-species Rydberg molecules using optical tweezers, Phys. Rev. Lett. **134**, 133401 (2025).
[65] D. Jaksch, J. I. Cirac, P. Zoller, S. L. Rolston, R. Côté, and M. D. Lukin, Fast quantum gates for neutral atoms, Phys. Rev. Lett. **85**, 2208 (2000).
[66] M. D. Lukin, M. Fleischhauer, R. Cote, L. M. Duan, D. Jaksch, J. I. Cirac, and P. Zoller, Dipole blockade and quantum information processing in mesoscopic atomic ensembles, Phys. Rev. Lett. **87**, 037901 (2001).
[67] C. Ates, T. Pohl, T. Pattard, and J. M. Rost, Antiblockade in Rydberg excitation of an ultracold lattice gas, Phys. Rev. Lett. **98**, 023002 (2007).
[68] T. Amthor, C. Giese, C. S. Hofmann, and M. Weidemüller, Evidence of antiblockade in an ultracold Rydberg gas, Phys. Rev. Lett. **104**, 013001 (2010).

End Matter

Appendix A: Charge-dipole mediated resonant monopole-dipole transition—The resonant monopole-dipole energy transfer reported here has, to our knowledge, not been previously described, warranting further discussion. With a more comprehensive model provided in Supplementary Material [42], we present an effective two-channel model in this appendix to elucidate the core physics of the RET process. During a two-body collision, the Hamiltonian in the center of mass frame of the collision complex is

$$H = H_0 + V_{\mathrm{CD}}(\boldsymbol{r}, \boldsymbol{R}) = H_{\mathrm{He}} + H_{\mathrm{NH_3}} + \frac{\boldsymbol{P}^2}{2\mu} + V_{\mathrm{CD}}(\boldsymbol{r}, \boldsymbol{R}), \tag{A1}$$

where $\boldsymbol{P}$ is the relative momentum of the He atom and the NH_3 molecule, and $\mu = m_{\mathrm{He}} m_{\mathrm{NH_3}}/(m_{\mathrm{He}} + m_{\mathrm{NH_3}})$ is the reduced mass of the collision partners. In the combined atom-molecule Hilbert space, it is most natural to employ the basis in which the noninteracting

Hamiltonian $(H_{\mathrm{He}}+H_{\mathrm{NH_3}})|n\ell m_\ell\rangle|\Pi\rangle = E_\Pi^{n\ell m_\ell}|n\ell m_\ell\rangle|\Pi\rangle$, where $E_\Pi^{n\ell m_\ell}$, the sum of corresponding noninteracting He and NH_3 energies is diagonal, to construct a matrix representation of $V_{\mathrm{CD}}(\boldsymbol{R})$. In doing so, we ignore the molecular rotational structure by virtue of an adiabatic approximation (see [42] and references therein for further details).

In this situation, because all other states are energetically much further detuned compared to their splitting, we adopt a minimal model by truncating our basis set to just the following two states:

$$|\downarrow\rangle = |65\mathrm{s}, -\rangle, \tag{A2a}$$

$$|\uparrow\rangle = |66\mathrm{s}, +\rangle. \tag{A2b}$$

The resulting interaction matrix is given by

$$\boldsymbol{V}_{\mathrm{CD}}(\boldsymbol{R}) = \begin{pmatrix} \langle\downarrow|V_{\mathrm{CD}}(\boldsymbol{R})|\downarrow\rangle & \langle\downarrow|V_{\mathrm{CD}}(\boldsymbol{R})|\uparrow\rangle \\ \langle\uparrow|V_{\mathrm{CD}}(\boldsymbol{R})|\downarrow\rangle & \langle\uparrow|V_{\mathrm{CD}}(\boldsymbol{R})|\uparrow\rangle \end{pmatrix}, \tag{A3}$$

with matrix elements

$$\begin{aligned}&\langle\Pi'|\langle n'\mathrm{s}|V_{\mathrm{CD}}(\boldsymbol{R})|n\mathrm{s}\rangle|\Pi\rangle \\ &\approx -\frac{e\langle\Pi'||\mu_{\mathrm{NH_3}}||\Pi\rangle}{R^2}\int_0^R r^2\mathrm{d}r\mathcal{R}_{n'\mathrm{s}}(r)\mathcal{R}_{n\mathrm{s}}(r)\cos\theta_R,\end{aligned} \tag{A4}$$

as shown in Fig. 4, where $\theta_R = \cos^{-1}(\hat{\boldsymbol{\mu}}_{\mathrm{NH_3}}\cdot\hat{\boldsymbol{R}})$ is the angle between the molecular dipole and collision axis, and $\mathcal{R}_{n\mathrm{s}}(r)$ are the Rydberg state radial wave functions. Importantly, while the radial wave functions are orthogonal over the entire radial domain $\int_0^\infty \mathcal{R}_{n'\ell'}(r)\mathcal{R}_{n\ell}(r)r^2\mathrm{d}r = \delta_{n',n}\delta_{\ell',\ell}$, the overlap for $|n'\mathrm{s}\rangle$ and $|n\mathrm{s}\rangle$ states is generally nonzero over a finite region of $r < R$. This point makes clear the necessity for the molecule to enter the Rydberg electron charge distribution for resonant monopole-dipole energy transfer to occur. Under these conditions, for the triplet $\ell = 0$ Rydberg states in He with an energy splitting that is close to resonance with the NH_3 inversion interval, the monopole term in the expansion, for which $r < R$, dominates. When integrated over this finite range, up to the position of the molecule, this term is nonzero.

Finally, regarding the scattering process, we can further expand the collisional angular momentum in partial waves $|L, m_L\rangle$,

$$\begin{aligned}&\langle L', m_L'|\langle\Pi'|\langle n'\mathrm{s}|V_{\mathrm{CD}}(\boldsymbol{R})|n\mathrm{s}\rangle|\Pi\rangle|L, m_L\rangle \\ &\quad\approx -\frac{e\langle\Pi'||\mu_{\mathrm{NH_3}}||\Pi\rangle}{R^2}\int_0^R r^2\mathrm{d}r\mathcal{R}_{n'\mathrm{s}}(r)\mathcal{R}_{n\mathrm{s}}(r) \\ &\quad\times(-1)^{m_L'}\sqrt{(2L'+1)(2L+1)} \\ &\quad\times\begin{pmatrix} L' & 1 & L \\ -m_L' & 0 & m_L \end{pmatrix}\begin{pmatrix} L' & 1 & L \\ 0 & 0 & 0 \end{pmatrix},\end{aligned} \tag{A5}$$

where the 2×3 arrays denote Wigner 3-j symbols. This expansion makes it clear, through the selection rule $L' = L \pm 1$, that a collision must induce a single-quanta change of collisional angular momentum for each partial wave, changing its parity along with the parity of the NH_3 inversion sublevel. The total parity of the collision complex therefore remains conserved during the resonant monopole-dipole energy transfer process.

Appendix B: Experimental details—The conditions under which the experiments were performed, were similar to those employed previously to study resonant dipole-dipole interactions between Rydberg He atoms and NH_3 in Refs. [20,37]. In the present experiments, the region in which the atoms were laser photoexcited to Rydberg states, interacted with the molecules, and were detected by state-selective electric field ionization was located between two parallel copper electrodes separated by 1.43 cm.

To measure and minimize stray electric fields in the region between these electrodes, microwave spectra of the single-color two-photon $|65\mathrm{s}\rangle \rightarrow |63\mathrm{s}\rangle$ transition were recorded with a pure beam of He. In this process, 2-μs-duration pulses of microwave radiation were applied 1, 3, or 5 μs after Rydberg state photoexcitation, before detection by electric field ionization. These spectra were recorded with a range of offset potentials applied to one of the copper electrodes. The offset potential required to minimize the Stark shift of the transition was determined from these measurements, and then applied to compensate the stray field. For the pure beam of He atoms, the residual Stark shift of the $|65\mathrm{s}\rangle \rightarrow |63\mathrm{s}\rangle$ transition under these conditions indicated that the remaining uncancelled stray electric field was ∼13 mV/cm.

In the measurements presented in Fig. 3, to state-selectively probe atoms in the $|66\mathrm{s}\rangle$ state that had undergone resonant energy transfer in a collision with an NH_3 molecule, the slightly larger residual stray electric field of 16.5 ± 4.5 mV/cm was determined with the molecules present in the beam. This stray field mixes < 0.03% of $|n\mathrm{p}\rangle$ character into the $|n\mathrm{s}\rangle$ states in He for $n \approx 65$. Since, for example, the single-photon $|65\mathrm{s}\rangle \rightarrow |66\mathrm{p}\rangle$ and $|65\mathrm{p}\rangle \rightarrow |66\mathrm{s}\rangle$ transitions have electric dipole transition moments of $115\,ea_0$ (295 D) and $1655e\,a_0$ (4205 D), respectively, the dominant contribution to an electric dipole transition moment between the ℓ-mixed $|65\mathrm{s}'\rangle$ and $|66\mathrm{s}'\rangle$ states in a weak stray electric field results from the $|65\mathrm{p}\rangle$ amplitude of $\sqrt{0.0003} = 0.017$ in the lower state. This yields an electric dipole moment for the single-photon $|65\mathrm{s}'\rangle \rightarrow |66\mathrm{s}'\rangle$ transition in a 16.5 mV/cm electric field of $\sim 30\,ea_0$ (75 D).

From the work reported in Ref. [20], we determined that an electric dipole transition moment of $1285e\,a_0$ (3265 D) resulted in ∼10% population transfer from the 40s state to the 40p state as a result of the resonant dipole-dipole interaction with the NH_3 molecules. In the work reported here on resonant monopole-dipole energy transfer, at

similar collision speeds and for comparable molecule number densities, we observe ∼17% population transfer. Because the electric dipole transition moments induced by ℓ mixing in the weak residual stray electric field in the experiments are $< 2.5\%$ of those encountered in the studies of resonant dipole-dipole interactions at lower values of n, they cannot be primarily responsible for the energy transfer observed here.